

Different Mechanisms Govern the Two-Phase Brust–Schiffrin Dialkylditelluride Syntheses of Ag and Au Nanoparticles

Ying Li,^{†,§} Oksana Zaluzhna,[†] Christopher D. Zangmeister,[‡] Thomas C. Allison,[‡] and YuYe J. Tong^{*,†}

[†]Department of Chemistry, Georgetown University, 37th and O Streets, NW, Washington, D.C. 20057, United States

[‡]National Institute of Standards and Technology, 100 Bureau Drive, Stop 8320, Gaithersburg, Maryland 20899-8320, United States

S Supporting Information

ABSTRACT: Here we report the first unambiguous identification of the chemical structures of the precursor species involving metal (Au and Ag) ions and Te-containing ligands in the Brust–Schiffrin syntheses of the respective metal nanoparticles, through which the different reaction pathways involved are delineated.

The two-phase Brust–Schiffrin method (BSM) for synthesizing dodecanethiolate-protected gold nanoparticles (NPs), which was published in 1994,¹ opened a new paradigm for rather facile syntheses of small (<5 nm) metal NPs stabilized by organic ligands whose yield could reach the gram level. Most research has focused on thiolate-protected metal NPs,^{2–10} in which sulfur acts as an anchoring element of the capping ligands that bind to the metal core. Quantum calculations have suggested that if heavier chalcogens (e.g., Se or Te) were used as the anchors, they would increase the conductance between the metal and the anchored ligand,¹¹ a parameter that is critically important in developing molecular electronics.¹² However, as in two-dimensional (2D) self-assembled monolayers (SAMs) on metal surfaces, there have been only a few studies of metal NPs protected by Te-containing ligands,^{13–15} which are the 3D analogues of the 2D SAMs. The first synthesis of Au NPs protected by Te-containing ligands was reported by Brust et al.,¹⁵ but their NPs were unstable, allowing no characterization other than a Langmuir isotherm plot.

Our group previously reported successful syntheses of stable Au NPs using $(C_8H_{17}Te)_2$ as a ligand precursor through the BSM¹⁴ and its later improvement.¹³ In terms of the corresponding Au NP formation chemistry, it was initially conjectured that polymeric $[Au(I)-TeR]_n$ species were formed before the final reduction to Au NPs.¹⁴ This was based on the observation of a colorless solution obtained after mixing of $(RTe)_2$ with a Au(III) solution analogous to that obtained after adding RSH to a typical wine-red Au(III) solution. The consensus at that time was that the latter consisted of polymeric $[Au(I)-SR]_n$.^{9,10} However, more recent work by Goulet and Lennox¹⁶ and by us^{13,17} showed that the intermediate species of Au ions in a typical BSM synthesis with thiols is not polymeric $[Au(I)-SR]_n$ but rather a $[TOA^+][Au(I)X_2]$ complex (TOA^+ = tetraoctylammonium cation; X = Cl, Br). This led us to revisit the conjecture of polymeric $[Au(I)TeR]_n$ species in the BSM synthesis of tellurate-protected Au NPs simply because a clear identification of the chemical structures of the precursor species

involving metal ions and Te-containing ligands would provide mechanistic information that is critical for the control of the size and size distribution of the synthesized metal NPs.^{17,18}

In this communication, we report ¹H NMR, Raman, and X-ray photoelectron spectroscopy (XPS) investigations of reaction intermediates aided by density functional theory (DFT) calculations that have enabled us to determine the chemical structures of the species involved. The reaction intermediates were prepared by adding $(RTe)_2$ to the benzene layer of Au(III) or Ag(I) after phase transfer with tetraoctylammonium bromide (TOAB). In the typical BSM synthesis, we found that $(RTe)_2$ reduced Au(III) to Au(I) with no formation of a Te–Au bond, while no reaction occurred at all between $(RTe)_2$ and Ag(I).

Specifically, the intermediate solutions were prepared as follows. For the synthesis of Au NPs, 0.07 mL of HAuCl₄ aqueous solution (0.1421 M) was mixed with 0.03 mmol of TOAB in 0.8 mL of benzene (or C₆D₆). After the mixture was stirred for 30 min, the organic layer was collected, and 0.0033 mmol of $(C_{12}H_{25}Te)_2$ dissolved in 0.2 mL of benzene (or C₆D₆) was added to the preprepared organic layer. The initial wine-red color of the solution started fading away. After the mixture was stirred for 1 h, a clear, colorless intermediate solution was obtained. The amount of $(RTe)_2$ used was critically important. When less $(RTe)_2$ was used, the solution turned yellow; when more $(RTe)_2$ was used, an unstable brown solution formed that led to a golden precipitate. For the synthesis of Ag NPs, 1 mmol of AgNO₃ was dissolved in 1 mL of H₂O and then mixed with 3 mmol of TOAB dissolved in 25 mL of benzene. After the mixture was vigorously stirred overnight, a two-layer, clear, colorless solution was obtained. That all of the Ag(I) ions had been transferred to the organic layer was verified by addition of NaBH₄ powder to the separated bottom aqueous layer, whereupon no color change or reaction was observed. The top organic layer was collected as a Ag(I) stock solution (0.04 M). $(C_{12}H_{25}Te)_2$ (0.025 mmol) was dissolved in 0.49 mL of benzene (or C₆D₆) and then added to 0.310 mL of Ag(I) stock solution, and the color of the mixture changed to slightly yellow. After the solution was vigorously stirred for 1 h, no color change occurred, and a clear yellow intermediate solution was obtained. The solvent was removed by rotary evaporation, and the dried intermediates were used for Raman and XPS measurements. The fresh dried intermediates could be redispersed well in benzene. In cases

Received: November 17, 2011

Published: January 17, 2012

where C_6D_6 was used as the solvent, the intermediate solutions were used for 1H NMR studies. Finally, after addition of 10 equiv of $NaBH_4$ to the two intermediate solutions, 3.44 ± 0.51 nm Au NPs and 2.86 ± 0.30 nm Ag NPs were obtained [Figure S1 in the Supporting Information (SI)].

The Raman spectra of the Au system intermediate [i.e., $3TOAB + HAuCl_4 + 0.33(C_{12}H_{25}Te)_2$] (Figure 1a), the pure

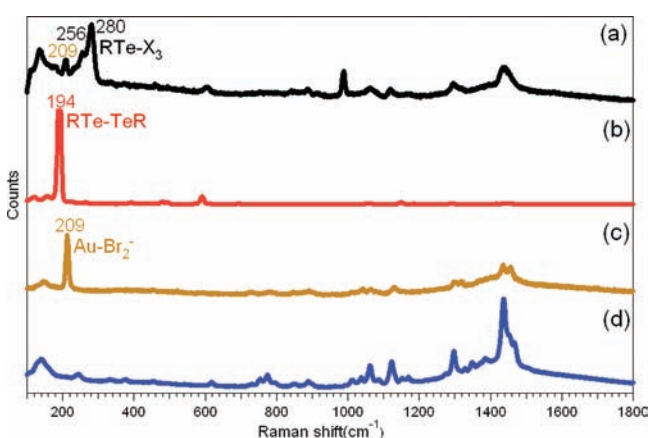


Figure 1. Raman spectra of (a) dried intermediate of the Au system [i.e., $3TOAB + HAuCl_4 + 0.33(C_{12}H_{25}Te)_2$], (b) $(C_{12}H_{25}Te)_2$, (c) $[TOA][AuBr_2]$, and (d) TOAB.

ligand (Figure 1b), TOAB (Figure 1d), and a reference compound ($[TOA][AuBr_2]$) are shown in Figure 1. Upon comparison with the spectrum of $(C_{12}H_{25}Te)_2$ (Figure 1b), the peak at 194 cm^{-1} , which can be assigned to the $RTe-TeR$ vibration according to our DFT calculations (see Table S1 in the SI), was found to be absent from the spectrum of the intermediate (Figure 1a). The absence of this vibrational band indicates that $(RTe)_2$ reacted with Au(III). Upon comparison with the reference spectra (Figure 1c,d), the peaks in the spectrum of the intermediate from $Au(I)Br_2^-$ (209 cm^{-1}),^{13,19} TOAB, and benzene (991 cm^{-1}), respectively, can be identified first. Interestingly, no peak due to the vibration of $Te-Au$ (see the SI) appears in the spectrum of the intermediate. This implies that no $Te-Au$ bonding occurred in the intermediate, which is very similar to what we have observed in the BSM synthesis of thiolate-protected Au NPs.¹³ Therefore, we propose that the Au ions after the addition of $(RTe)_2$ were in the form of $[TOA][AuX_2]$, as identified in the thiol systems.^{13,17,18} In regard to the broad peak at 280 cm^{-1} , our DFT calculations (Table S1) suggest that it has to do with $Te-X$ ($X = Cl, Br$) vibrations (dominated by those of $Te-Cl$ in terms of Raman intensity).

Figure 2 (for the spectra with full peaks, see Figure S2) presents the 1H NMR spectra of the corresponding Au intermediate solution (Figure 2a), the separated organic layer right after phase transfer ($3TOAB + HAuCl_4$) (Figure 2b), pure ligand $(C_{12}H_{25}Te)_2$ (Figure 2c), and the solution obtained by adding 2 equiv of $C_{12}H_{25}SH$ to the solution in (b) (Figure 2d). In addition to the peaks of $[TOA^+]$ (see the SI for the chemical shift values), Figure 2b contains most noticeably a peak at 2.63 ppm from encapsulated water.¹⁷ The addition of $(C_{12}H_{25}Te)_2$ to the organic layer of Figure 2b led to the intermediate solution of Figure 2a, where the characteristic proton peak of ditelluride at 2.95 ppm (Figure 2c) disappeared. The latter observation indicates that the $Te-Te$ bond was broken, which is consistent with the Raman results pointing to $Te-Te$ bond

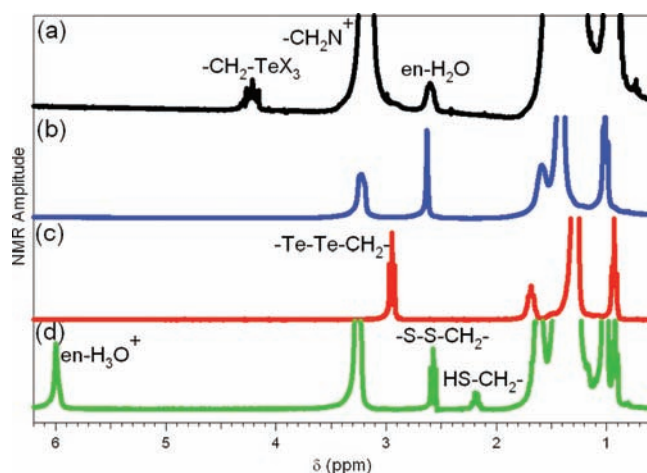


Figure 2. 1H NMR spectra (in C_6D_6) of (a) the intermediate solution of the Au system [i.e., $3TOAB + HAuCl_4 + 0.33(C_{12}H_{25}Te)_2$], (b) the organic phase after phase transfer (i.e., $3TOAB + HAuCl_4$), (c) $(C_{12}H_{25}Te)_2$, and (d) the solution formed by addition of 2 equiv of $C_{12}H_{25}SH$ to the solution in (b). The concentration of each chemical was kept the same in all samples.

breaking after the addition of $(RTe)_2$ to the organic layer containing Au(III).

That the wine-red-colored Au(III) solution became colorless after the addition of $(RTe)_2$ indicates a reduction of Au(III) to Au(I). However, comparison with Figure 2d, which is the spectrum of the solution obtained by adding 2 equiv of thiol to the solution of Figure 2b, shows that the intermediate does not contain encapsulated H_3O^+ , indicating that no proton/water was involved in the reaction. On the other hand, the Raman data and DFT calculations suggest the formation of a $Te-halide$ bond, implying that the Te acts as a reductant, which was further confirmed by the XPS measurements carried out on the dried intermediate (Figure 3).

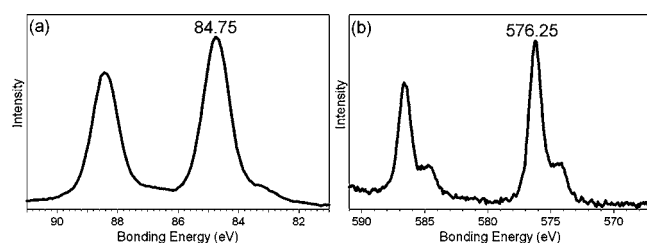
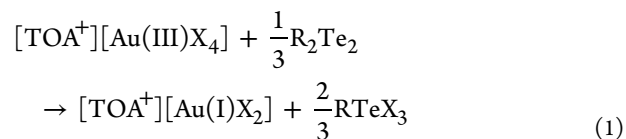


Figure 3. (a) Au 4f and (b) Te 3d XPS spectra of the dry intermediate of the Au system [i.e., $3TOAB + HAuCl_4 + 0.33(C_{12}H_{25}Te)_2$].

On the basis of the available literature values for Au(I),^{20,21} the Au 4f peak at 84.75 eV in Figure 3a confirms that the oxidation state of the Au ion in the intermediate is indeed +1. Moreover, the Te 3d peak at 576.25 eV agrees with the reported Te 3d binding energy of $C_4H_9TeBr_3$,²² which suggests that the oxidation state of Te is +2. Therefore, we propose the following stoichiometric reaction for the reduction of Au(III) to Au(I) by the ditelluride, whose oxidation state changes accordingly from -1 to $+2$:

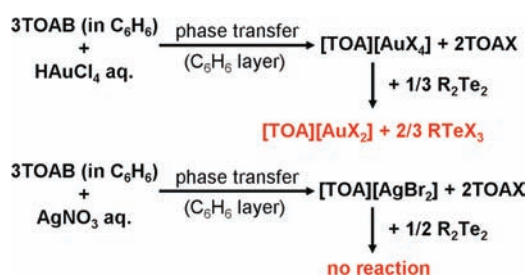


where X represents a halide. The presence of RTeX_3 as a product of eq 1 was further confirmed by the observation of a new ^1H peak at 4.21 ppm in Figure 2a that can be assigned to $\alpha\text{-CH}_2$ in $\text{C}_{12}\text{H}_{25}\text{TeX}_3$ on the basis of the reported chemical shift of $\alpha\text{-CH}_2$ in $\text{C}_2\text{H}_5\text{TeCl}_3$.^{23–25}

For comparison, we also investigated the BSM intermediate of a Ag system with $(\text{RTe})_2$. Its ^1H NMR spectrum (Figure S3a) appears to be a linear combination of the spectra of the individual components, namely, the organic layer after the phase transfer of AgNO_3 with 3 equiv of TOAB (Figure S3b) and the added R_2Te_2 (Figure S3c). The characteristic proton peak of ditelluride at 2.95 ppm remained intact in the spectrum of the intermediate, and no new peaks were observed. This indicates that $(\text{RTe})_2$ did not react with Ag(I) , a conclusion that is further supported by analysis of the Raman spectra (Figure S4). The Raman spectrum of the intermediate (Figure S4a) is clearly also a linear combination of those of the individual components, the RTe-TeR vibration at 194 cm^{-1} (Figure S4b) and the Ag(I)Br_2^- vibration at 147 cm^{-1} (Figure S4c). No new Raman peaks were observed. That is, no reaction took place between the added $(\text{RTe})_2$ and the Ag ions in $[\text{TOA}^+][\text{Ag(I)Br}_2^-]$.

In summary, we have identified the chemical structures of the intermediate species of both Te-containing ligand and metal ions (Au or Ag) when $(\text{RTe})_2$ is used in place of thiol in a typical BSM synthesis. Via careful and detailed ^1H NMR, Raman, and XPS characterizations as well as comparison to DFT calculations of the reaction intermediates obtained in typical BSM syntheses before the addition of NaBH_4 , we conclude that for the Au system, the added $(\text{RTe})_2$ reduces Au(III) to Au(I) with concurrent Te–Te bond breaking and the formation of RTeX_3 (eq 1). However, no formation of a Au–Te bond was observed. For the Ag system, on the other hand, no evidence of a reaction between Ag(I) and $(\text{RTe})_2$ could be observed. The aforementioned difference is summarized in Scheme 1. We believe that these new

Scheme 1. Chemical Behavior of $(\text{RTe})_2$ in the BSM Syntheses of Au and Ag NPs



mechanistic insights will open the door to the exploration of ligand-protected metal NPs with Te as an anchoring element.

■ ASSOCIATED CONTENT

Supporting Information

Experimental and synthetic details, optimized structures from DFT calculations, TEM images with UV–vis spectra and size distribution plots, and ^1H NMR and Raman spectra of the intermediate of the Ag system. This material is available free of charge via the Internet at <http://pubs.acs.org>.

■ AUTHOR INFORMATION

Corresponding Author

yyt@georgetown.edu

Present Address

[§]Department of Medicine, Georgetown University Medical Center, 3800 Reservoir Road, NW, Washington, D.C. 20007.

Notes

The authors declare no competing financial interest.

■ ACKNOWLEDGMENTS

This work was supported by grants from the NSF (CHE-0456848 and CHE-0923910). The authors thank the UMD NISP Lab for use of its TEM facility. A portion of the research was performed using EMSL, a National Scientific User Facility sponsored by the Department of Energy's Office of Biological and Environmental Research and located at Pacific Northwest National Laboratory.

■ REFERENCES

- (1) Brust, M.; Walker, M.; Bethell, D.; Schiffrin, D. J.; Whyman, R. J. *Chem. Soc., Chem. Commun.* **1994**, 801.
- (2) Collier, C. P.; Saykally, R. J.; Shiang, J. J.; Henrichs, S. E.; Heath, J. R. *Science* **1997**, *277*, 1978.
- (3) Heath, J. R.; Knobler, C. M.; Leff, D. V. *J. Phys. Chem. B* **1997**, *101*, 189.
- (4) Chen, S.; Huang, K.; Stearns, J. A. *Chem. Mater.* **2000**, *12*, 540.
- (5) Chen, S.; Sommers, J. M. *J. Phys. Chem. B* **2001**, *105*, 8816.
- (6) Lica, G. C.; Zelakiewicz, B. S.; Tong, Y. Y. *J. Electroanal. Chem.* **2003**, *554–555*, 127.
- (7) Zelakiewicz, B. S.; de Dios, A. C.; Tong, Y. Y. *J. Am. Chem. Soc.* **2003**, *125*, 18.
- (8) Zelakiewicz, B. S.; Lica, G. C.; Deacon, M. L.; Tong, Y. Y. *J. Am. Chem. Soc.* **2004**, *126*, 10053.
- (9) Funston, A. M.; Mulvaney, P.; Murray, R. W. *Langmuir* **2009**, *25*, 13840.
- (10) Jin, R. *Nanoscale* **2010**, *2*, 343.
- (11) Di Ventra, M.; Lang, N. D. *Phys. Rev. B* **2001**, *65*, No. 045402.
- (12) Cheng, Z. L.; Skouta, R.; Vazquez, H.; Widawsky, J. R.; Schneebeli, S.; Chen, W.; Hybertsen, M. S.; Breslow, R.; Venkataraman, L. *Nat. Nanotechnol.* **2011**, *6*, 353.
- (13) Li, Y.; Zaluzhna, O.; Xu, B.; Gao, Y.; Modest, J. M.; Tong, Y. Y. *J. Am. Chem. Soc.* **2011**, *133*, 2092.
- (14) Li, Y.; Silverton, L. C.; Haasch, R.; Tong, Y. Y. *Langmuir* **2008**, *24*, 7048.
- (15) Brust, M.; Stühr-Hansen, N.; Norgaard, K.; Christensen, J. B.; Nielsen, L. K.; Bjørnholm, T. *Nano Lett.* **2001**, *1*, 189.
- (16) Goulet, P. J. G.; Lennox, R. B. *J. Am. Chem. Soc.* **2010**, *132*, 9582.
- (17) Li, Y.; Zaluzhna, O.; Tong, Y. Y. *Langmuir* **2011**, *27*, 7366.
- (18) Li, Y.; Zaluzhna, O.; Tong, Y. Y. *J. Chem. Commun.* **2011**, *47*, 6033.
- (19) Braunstein, P.; Clark, R. J. H. *J. Chem. Soc., Dalton Trans.* **1973**, 1845.
- (20) McNeillie, A.; Brown, D. H.; Smith, W. E.; Gibson, M.; Watson, L. *J. Chem. Soc., Dalton Trans.* **1980**, 767.
- (21) Kitagawa, H.; Kojima, N.; Nakajima, T. *J. Chem. Soc., Dalton Trans.* **1991**, 3121.
- (22) Bahl, M. K.; Watson, R. L.; Irgolic, K. J. *J. Chem. Phys.* **1977**, *66*, 5526.
- (23) Wynne, K. J.; Pearson, P. S. *Inorg. Chem.* **1971**, *10*, 2735.
- (24) Wynne, K. J.; Pearson, P. S. *Inorg. Chem.* **1971**, *10*, 1871.
- (25) Irgolic, K. J. *The Organic Chemistry of Tellurium*; Gordon & Breach: New York, 1974.